Energy-resolved positron annihilation for molecules

L. D. Barnes, S. J. Gilbert, and C. M. Surko
Department of Physics, University of California, San Diego, California 92093-0319
(Received 22 October 2002; published 17 March 2003)

This paper presents an experimental study designed to address the long-standing question regarding the origin of very large positron annihilation rates observed for many molecules. We report a study of the annihilation, resolved as a function of positron energy ($\Delta E \sim 25$ meV, full width at half maximum) for positron energies from 50 meV to several eV. Annihilation measurements are presented for a range of hydrocarbon molecules, including a detailed study of alkanes, C_nH_{2n+2}, for $n=1-9$ and 12. Data for other molecules are also presented: C_2H_2, C_2H_4; CD_4; isopentane; partially fluorinated and fluorinated methane (CH_xF_{4-x}); 1-fluorohexane ($C_6H_{13}F$) and 1-fluorononane ($C_9H_{19}F$). A key feature of the results is very large enhancements in the annihilation rates at positron energies corresponding to the excitation of molecular vibrations in larger alkane molecules. These enhancements are believed to be responsible for the large annihilation rates observed for Maxwellian distributions of positrons in molecular gases. In alkane molecules larger than ethane (C_2H_6), the position of these peaks is shifted downward by an amount ~ 20 meV per carbon. The results presented here are generally consistent with a physical picture recently considered in detail by Gribakin [Phys. Rev. A **61**, 022720 (2000)]. In this model, the incoming positron excites a vibrational Feshbach resonance and is temporarily trapped on the molecule, greatly enhancing the probability of annihilation. The applicability of this model and the resulting enhancement in annihilation rate relies on the existence of positron-molecule bound states. In accord with this reasoning, the experimental results presented here provide the most direct evidence to date that positrons bind to neutral molecules. The shift in the position of the resonances is interpreted as a measure of the binding energy of the positron to the molecule. Other features of the results are also discussed, including large, qualitative changes in the annihilation spectra observed when hydrocarbon molecules are fluorinated.

DOI: 10.1103/PhysRevA.67.032706 PACS number(s): 34.85.+x, 34.50.−s, 78.70.Bj, 71.60.+z

I. INTRODUCTION

As low-energy positrons become more easily available in the laboratory, understanding of the interaction of positrons with matter will become increasingly important. More accurate models of positron-molecule interactions could benefit research in such varied areas as interpretation of astrophysical gamma-ray spectra [1], positron-induced fragmentation of molecules [2,3], and characterization of thin films and material surfaces [4,5]. In addition, positron-matter interactions pose a number of challenges to our fundamental understanding of atomic physics [6,7]. Much recent research has been directed toward finding methods to treat electron-positron correlations and positronium formation as either an open or closed channel for theoretical calculations of elastic and inelastic cross sections as well as annihilation rates [8–12].

In this paper, we focus on a question in this area which has remained unanswered for nearly four decades. In 1963, measurements by Paul and Saint-Pierre indicated unusually high annihilation rates for positrons incident on certain large molecules even though the positron energy was below the energy threshold for positronium formation [13]. While several explanations have been advanced to explain this phenomenon, clear experimental confirmation of the predictions of any model has been lacking [8-10,14-18].

We present studies of the annihilation rate for positrons incident on a sampling of molecules resolved as a function of positron energy. These measurements are made using a recently developed technique for the creation of a positron beam which is tunable in energy from 50 meV to several eV with an energy spread of $\simeq$ 25 meV (full width at half maximum) [19,20]. This beam has previously been used to study elastic and inelastic scattering of positrons [21–24]. The present study here focuses on positron annihilation rates. The data presented provide evidence that molecular vibrations are intimately connected with the observed large annihilation rates, and point to vibrational-excitation mediated trapping into positron-molecule bound states (i.e., vibrational Feshbach resonances) as the specific mechanism of the enhancement.

The magnitude and energy dependence of these rates are explored for alkanes (C_nH_{2n+2}) up to dodecane ($n=12$), alkenes and alkynes, deuterated alkanes, fluorinated alkanes, and nonlinear carbon chain molecules. The results provide important guidance for theoretical attempts to explain the mechanism responsible for these large rates and should lead to a firmer understanding of positron-molecule interactions. Some of the work presented here was reported previously in Ref. [25].

Annihilation rates for positrons in molecular gases are typically expressed in terms of the dimensionless parameter, Z_{eff}, given by

$$Z_{eff}=\Gamma/(\pi r_0^2 c n_m), \tag{1}$$

where Γ is the measured annihilation rate for positrons in the test gas, r_0 is the classical electron radius, c is the speed of light, and n_m is the molecular density. Ignoring correlations between the positron and molecular electrons, Γ would be

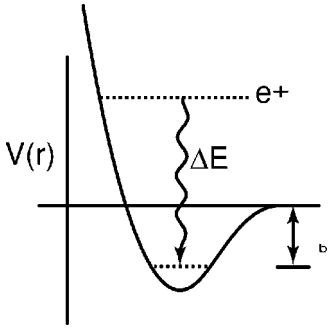

FIG. 1. A semiclassical picture of resonant annihilation enhancement of Z_{eff}. A positron approaching the molecule can fall into a bound state of binding energy ε_b by the excitation of an electronic or vibrational transition of energy $\Delta E = E_{ex} - E_0$. Bound positrons have large overlap with molecular electrons compared to free positrons leading to a large increase in the annihilation rate.

equal to the Dirac rate, $\pi r_0^2 c n_m Z$, with Z as the number of electrons per molecule. In such an uncorrelated model, Z_{eff} is predicted to be equal to Z. Actual measurements for positrons at energies near room temperature (300 K $\simeq 0.025$ eV) show that, in some cases, Z_{eff} is orders of magnitude larger than Z [13,18]. Octane, for example, with a Z of 66, has a Z_{eff} of 6×10^5. Annihilation rates are found to increase rapidly with molecular size. Values of $Z_{eff} = 10^7$ are observed for alkanes only twice as large as octane.

Several theoretical models have been proposed to explain this phenomenon in terms of a vibrational or electronic resonance or a positron-molecule bound state [14–18]. In these models, a long-lived quasibound state can increase the overlap of the positron and electron wave functions and enhance the probability of annihilation. Explanations have been advanced involving the excitation of virtual positronium and other mechanisms involving very strong positron-electron correlations [9,10].

A model proposed by Gribakin [17,18] explains some of the important features of the observed rates and is useful in the discussion of the data presented here. This model distinguishes two mechanisms for the enhancement of Z_{eff}. *Direct annihilation* can make contributions to Z_{eff} up to ~ 1000. Enhancements to direct annihilation (first considered in Ref. [14]) occur when a shallow bound state or low-energy virtual state of the system exists. In this case, the positron density in the vicinity of the target is increased proportional to $1/(\varepsilon + |\varepsilon_0|)$, where ε is the incident energy and ε_0 is the energy of the weakly bound or virtual state. The annihilation parameter Z_{eff} is enhanced by the same factor. For positrons with finite energy, this mechanism is limited by the presence of ε in the denominator. Consequently, for room-temperature positrons, direct annihilation can make a contribution to Z_{eff} of no more than ~ 1000 [17].

The second type of enhancement, *resonant annihilation* (i.e., Feshbach resonance enhancement), illustrated in Fig. 1, occurs when the energy of the incident positron plus the energy of the ground state, neutral target molecule matches the energy of an excited quasistable positron-molecule bound state. This bound state can involve electronic or vibrational excitation of the target to account for energy given up by the positron falling into a bound state. When such a resonance occurs, the overlap between the positron wave function and those of the target electrons is greatly increased, resulting in a large value of Z_{eff}. Assuming that the presence of the positron has little effect on the excited (e.g., vibrational) states of the target [17], the condition on the incident positron energy for such a resonance to occur is

$$\varepsilon = E_{ex} - E_0 - \varepsilon_b, \tag{2}$$

where ε is the incident positron energy, E_{ex} is the energy of the excited state of the target, E_0 is the energy of the ground state of the target, and ε_b is the binding energy of the positron to the target. In the energy range of the data presented here, vibrational excitation is the important interaction.

II. PREVIOUS EXPERIMENTS

Most previous experimental work in this area used positrons in a thermal (Maxwellian) distribution at 300 K. While identifying important chemical trends, these studies have not conclusively established a mechanism responsible for these enhanced annihilation rates. In this paper, these Z_{eff} values measured using room-temperature thermal distributions of positrons will be referred to as Z_{eff} (300 K).

The earliest work in this area was done by introducing positrons into dense gases and observing the annihilation lifetime [13,15,26]. These experiments demonstrated the rapid increase in Z_{eff} with increasing molecular size.

Later experiments, which introduced thermal positron plasmas into low pressure gas, expanded the range of experiments to larger molecules and pointed out very strong dependences of Z_{eff} on chemical composition (e.g., fluorination) [16,27]. In work by Iwata *et al.* [18], measuring Z_{eff} for a heated Maxwellian distribution of positrons, Z_{eff} was found to vary as $T^{-1/2}$ for temperatures near 300 K, but to decrease more slowly at higher temperatures. It was postulated that this might be due to some structure at energies above 300 K, but below the threshold for positronium formation. Since all of these experiments used Maxwellian distributions of positrons, resolution of such structure in the annihilation spectrum was not possible. This requires a tunable, monochromatic low energy positron beam, such as that described in the next section.

III. EXPERIMENTAL SETUP

The experiments are performed using a buffer-gas trap technique [16,28] to accumulate and cool positrons to 300 K. The positrons are then electrostatically forced from the accumulator and magnetically guided ($B \sim 0.1$ T) through a cell filled with the gas to be studied as shown in Fig. 2. The energy of the positrons in the gas cell is defined by the potential on a cylindrical electrode. Annihilation radiation from the interaction of the positrons with the test gas is detected by a CsI scintillator. The positron beam is operated in a pulsed mode, with $\sim 10^4$ positrons per pulse at a repetition rate of 4 Hz. The number of positrons per pulse is determined by measuring the charge delivered to a collector plate at the far end of the apparatus. The positron energy distribu-

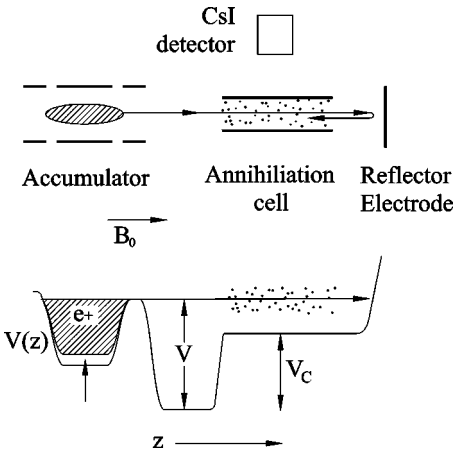

FIG. 2. Schematic diagram of the experiment (above), and corresponding electrical potential $V(z)$ as a function of position along the magnetic field (below). A cold positron beam is passed through a gas cell. The energy of the beam, $\varepsilon = e(V - V_c)$, can be tuned from 50 meV upward. To avoid background, the positrons are reflected back through the cell and kept in flight, passing back and forth through the cell, while annihilation events are recorded.

tion in the beam is approximately Gaussian with a width of $\simeq 25$ meV as measured using a retarding potential analyzer.

Figure 3 is a more detailed drawing of the apparatus. It shows the path of the positrons (dashed line) after they exit the accumulator. Cryo pumps maintain a base pressure of 10^{-9} torr in the vacuum chamber in the absence of the test gas. A pair of magnetic coils create a 0.1-T magnetic field in the gas cell while providing optical access for the detector. The gas cell and the detector are surrounded by 5 cm of lead to avoid detection of gamma rays from external sources. Copper baffles inside the vacuum chamber (*B* and *C* in Fig. 3) also provide shielding. The magnets, the detector, and the lead shielding are all external to the vacuum chamber.

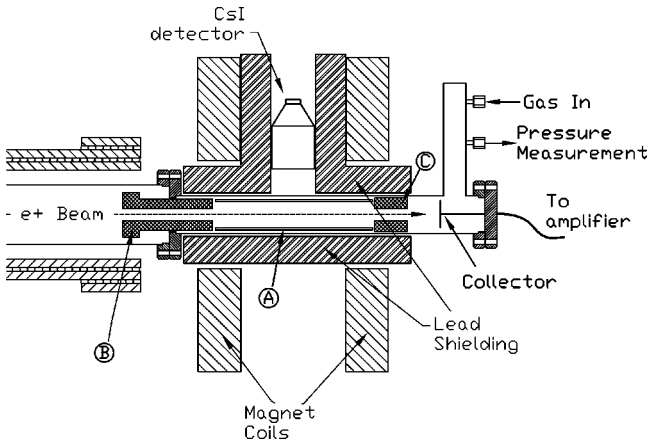

FIG. 3. Cut-away view of the annihilation apparatus. The dashed line is the path of the positrons through the cell. The copper baffles help to define a favorable pressure profile and to shield against sources of annihilation radiation outside the gas cell. Baffles *B* and *C* are biased to set the potential profile at the ends of the gas cell. In particular, baffle *C* can be biased positively to reflect positrons back through the gas cell rather than allow them to strike the collector.

Electrode *A*, located directly between the magnet coils, defines the positron energy in the region visible to the annihilation radiation detector. This electrode is also used as a retarding potential analyzer (RPA) to determine the energy of the positrons in this region. The uniformity of the potential in this region is verified using a time-of-flight technique. The potential is found to be constant to within ~ 10 meV [23]. In the magnetic field *B*, in the accumulator region ($B \simeq 0.9$ kG), the positron motion can be separated into a component along the magnetic field and the gyromotion of the positron in the plane perpendicular to *B*. Only the energy associated with positron motion parallel to the magnetic field, $E_\parallel$, is measured with the RPA. Energy associated with the perpendicular motion, $E_\perp$, is assumed to be 25 meV (i.e., 300 K) in the positron accumulator. This motion is confined to tiny cyclotron orbits, but is nonetheless important in collisions with the test gas. Since $E_\perp / B$ is an invariant for a slowly varying magnetic field, $E_\perp$ is reduced by a factor equal to the ratio of the magnetic field in the gas cell to that in the accumulator. Taking into account the magnetic-field ratio in our apparatus, we take $E_\perp$ in the gas cell to be 16 meV. The total positron energy is assumed to be 16 meV larger than that measured by the RPA.

The average positron energy in the region visible to the detector can be varied from 50 meV to ~ 100 eV. For positron energies below 50 meV, a significant fraction of the positrons, due to elastic collisions with the test gas, do not have sufficient kinetic energy in the direction of the magnetic field to enter the gas-filled region and are reflected from the cell. This prevents accurate measurements below 50 meV using the current apparatus.

The copper baffles on either side of this electrode serve a dual purpose. Baffle *B* serves to create a region of high test gas pressure inside the cell and lower pressure on the accumulator side of the baffle. Both baffles are electrically insulated from the cell electrode and the vacuum chamber and can therefore be biased to define the energy of positrons in the regions near the baffle. The baffle *B* on the accumulator side is biased to minimize elastic and inelastic scattering and annihilation in the region near this baffle. While the gamma-ray detector is only slightly sensitive to annihilation events in this region, an extremely large annihilation signal or large elastic or inelastic scattering in this higher pressure region could skew the measurement. Appropriate biasing of baffle *B* minimizes these effects. The baffle *C* on the collector side of the electrode *A* can be biased high enough (~ 8 V) to reflect the positrons back through the cell instead of allowing them to collide with the collector. This eliminates any background signal that might arise from positrons annihilating on the collector. This ''multiple pass'' operation will be discussed further below.

Gamma radiation from annihilation events in the cell are detected using a CsI scintillator and photodiode (Fig. 3). The face of the scintillator is located 5 to 10 cm from the center of the cell. The detector produces a current pulse in response to a gamma photon, the height of which is proportional to the photon energy. The detection efficiency for annihilation events in the gas cell is calibrated using a source of known

activity. Only photons with energy within a narrow range near 511 keV are counted as annihilation events. Multiple photons arriving within the decay lifetime of the detector (~ 1 μs) are interpreted by the system as a single photon with energy outside the acceptable range. For this reason, care must be taken to ensure that the number of such events is negligible.

To further reduce background counts, the event counter is ''gated'' to count only those events detected within a 15-μs period during which the positrons are kept in flight. This is especially important when operated in ''multiple pass'' mode. In this mode of operation, baffle C is biased high and the positrons remain in flight while the counter gate is on. They are allowed to collide with the collector only after the counter gate is turned off. The positrons make between two and five passes through the cell during the 15-μs detection time, depending on the energy of the positrons inside and outside the cell. This number of passes is calculated and taken into account in the determination of Z_{eff}. Using these techniques, the background (test gas pressure $<10^{-8}$ torr) signal is reduced to 1 count per 10^9 positrons.

Test gas pressure in the cell is determined using a capacitance manometer located a short distance from the cell and then calculating the pressure in the cell using the known conductances of the chambers and apertures. In the case of targets that are gaseous at room temperature, the pressure is maintained at a constant value by a needle valve controlled by a digital proportional-integral-differential (PID) controller using feedback from the capacitance manometer. Samples that are liquid at room temperature are maintained at a constant temperature using a PID controller, a thermocouple, and a Peltier cooling device. The vapor above the sample is allowed to flow into the gas cell through a manual needle valve adjusted to set the pressure in the cell. Test gas pressures range from 10^{-2} to 10^{-7} torr, and are adjusted to give signal levels on the order of 1 count per 10^6 positrons in a single transit through the cell. The detector position and positron pulse amplitude can also be adjusted slightly to produce signal levels that avoid multiple counts arriving simultaneously, but allow for reasonable data collection times.

Additionally, test gas pressure must be kept low enough to avoid introducing elastic or inelastic scattering effects. Where the elastic and inelastic cross sections for positrons are known, the test gas pressure is set so as to avoid scattering greater than 10% per pass. To verify that such scattering effects can be safely neglected, the gamma-ray signal for the first 15 μs was compared with the gamma-ray signal for the next 15 μs. The absence of statistically significant differences indicates that any changes to the number or energy of positrons in the pulse due to scattering during the first 15 μs had no significant effect on the annihilation signal.

The annihilation signal is found to be linear with test gas pressure indicating that the events measured are due to positrons interacting with at most one gas molecule and not interactions of a single positron with multiple molecules.

The quantity Z_{eff}, the annihilation rate normalized to the Dirac rate [Eq. (1)], can be calculated from the number of counts per pass using the measured detector efficiency, the energy of the positrons inside and outside the annihilation cell, the test gas pressure, and the average number of positrons per pulse. The efficiency of the detector is measured for varying source positions along the center line of the cell. This is done by counting gamma-ray photons from a radioactive source of known activity at varying positions along the path. An average of these values is used to calculate the average detector efficiency D over the cell length l given by

$$D=\frac{1}{l}\int_p f(x)dx, \tag{3}$$

where p indicates the straight path through the center of the cell, $f(x)$ is the measured efficiency as a function of position x, and l is the total cell length. This averaged efficiency D depends on the radial distance of the detector from the center of the cell. Measurements of D were made with the detector at several positions in order to be able to adjust D to increase or decrease the detected count rate. With this average efficiency, the cross section σ is given from the measured counts per positron per pass, N, and the target molecule density, n_m, by

$$\sigma=\frac{N}{n_m l D}. \tag{4}$$

When the apparatus is operated with the reflector electrode raised, the average number of times the positrons pass through the cell in the 15-μs window can be calculated from the length of the cell, the length of the positron path outside the cell, and the positron energy in both regions. For the data presented, this number of passes is usually between 2 and 5. The annihilation rate for positrons with velocity v is given by $\Gamma=\sigma n_m v$, and Z_{eff} can be calculated using

$$Z_{eff}=\frac{\Gamma}{\pi r_0^2 c n_m}=\frac{\sigma v}{\pi r_0^2 c}. \tag{5}$$

The error bars on the data in the figures shown here indicate only the random error. This random error is due primarily to statistical fluctuations in the number of annihilation events. Fluctuations in the size of the positron pulses are insignificant when averaged over many pulses.

The major sources of systematic error are the measurement of the pressure and the calibration of the measured pressure with the cell pressure, calibration of the amplifier used to measure the number of positrons per pulse, and possible changes in the average positron energy during multiple passes through the cell. The pressure measured by the capacitance manometer had small but noticeable fluctuations and a slight drift over time. Both of these effects are of the order of 10^{-6} torr. The capacitance manometer was used for pressures greater than 10^{-5} torr. For pressures below 10^{-5} torr, an ion gauge was used to measure pressure in the same region. Ion gauge sensitivity was measured in the system by comparing the measurements of the ion gauge and capacitance manometer. From this, we obtain ion gauge sensitivities estimated to be accurate to about $\pm 15\%$.

Additionally, there is systematic error in the measurement of the size of the positron pulses, primarily associated with

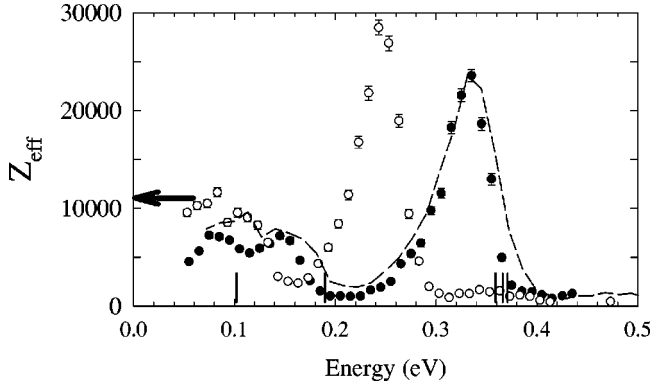

FIG. 4. Positron annihilation rate Z_{eff} as a function of incident positron energy for butane (●) and butane-d_{10} (○) in the range of energies $50 \leqslant \varepsilon \leqslant 450$ meV. Vertical bars show the energies of the strongest infrared-active vibrational modes for butane. Dashed line indicates Z_{eff} for butane-d_{10} appropriately scaled in energy by the reduced mass factor and scaled in amplitude to match the C-H peak for butane (see text). The arrow on the vertical axis indicates Z_{eff} for a room-temperature distribution of positrons incident on butane.

the calibration of the charge-sensitive amplifier used. The device was calibrated using a well-known input from a signal generator. We estimate the systematic error in the positron pulse size at 15%.

The total systematic error in the measurements of Z_{eff} presented here is therefore $\simeq 25\%$. This error is not expected to have a strong dependence on positron energy. Thus, while this systematic error may affect the overall scaling of the measured Z_{eff}, it is not expected to affect its dependence on positron energy.

While the present apparatus does not permit measurement of changes in the energy of positrons as they reflect from the reflector electrode, comparisons of measurements with and without the reflector agree to within 15 meV.

IV. RESULTS

A. Large alkanes

Early in the investigation of positron annihilation rates, it was found that the alkanes (C_nH_{2n+2}) and other hydrocarbon molecules exhibited very large annihilation rates. In the 1963 paper by Paul and Saint-Pierre, annihilation rates for *n*-butane, propane, and isobutane were reported [13]. Much research since that time focused on the alkanes and similar molecules [16,18,26]. Recently, the first energy-resolved measurements of Z_{eff} were reported [25]. Since the challenge of these experiments is distinguishing the annihilation signal due to positron-molecule interactions from external noise sources, the realtively large values of Z_{eff} in alkane molecules make them a natural place to begin.

Figure 4 shows Z_{eff} values for butane (C_4H_{10}) and butane-d_{10}(C_4D_{10}). Butane exhibits peaks in Z_{eff} in the region of the vibrational mode energies. In particular, a prominent peak ($Z_{eff} > 10^4$) appears for positron energies just lower than those of the C-H stretch vibrational modes. In the figure, the most prominent ir active modes are marked by vertical lines. At energies larger than the vibrational modes, Z_{eff} drops abruptly to much smaller levels, i.e., on the order of Z, the number of molecular electrons. For example, for butane ($Z=32$), Z_{eff} for positron energies between 0.5 and 3 eV is approximately 100 and is fairly constant. This is a drop in Z_{eff} of two orders of magnitude from the maximum Z_{eff} at the peak. Similar results are observed for the other alkanes.

To confirm that this enhancement is related to the vibrational modes of the molecule, the same Z_{eff} measurements were made for butane-d_{10}, a butane molecule with all of the hydrogen atoms substituted with deuterium, but having the same electronic structure. The C-H stretch modes are isolated from the rest of the vibrational spectrum and so this feature became the focus of our analysis of the Z_{eff} spectrum of the alkane molecules. Similar analysis of the other modes is possible. Deuteration reduces the energy of the C-H stretch mode by a factor equal to $\xi^{1/2}$, where $\xi = \mu_{\text{C-H}}/\mu_{\text{C-D}}$ is the ratio of the reduced masses associated with these vibrational modes. The reduced mass is different for each normal mode and can be determined from the motions of the nuclei in the mode. As a first approximation, the reduced mass for the stretching of an isolated C-H pair was used, which gives $\xi = 0.538$. The dashed line in Fig. 4 is data for butane scaled in energy by $\xi^{1/2}$ and scaled in magnitude for comparison. Not only the positions and shapes of the C-H (C-D) peaks, but the entire measured spectra agree quite well when scaled by this factor. From this analysis we conclude that these resonance peaks in the spectrum of the alkanes are related to one or several of the C-H stretch vibrational modes.

Figure 5 shows the energy resolved Z_{eff} spectrum for all of the alkanes measured. The energy dependence of Z_{eff} is largely the same as molecular size increases, but the magnitude of Z_{eff} increases rapidly and the resonances appear at an energy lowered by $\simeq 20$ meV for each carbon added. This downward shift is the strongest experimental evidence to date of positron binding to molecules. Figure 6 shows the position of the C-H stretch peak as a function of the number of carbons for the alkanes. Assuming the mode involved has an energy of 360 meV, we observe a shift of 205 meV for dodecane ($C_{12}H_{26}$) and a 10-meV upward shift for ethane (C_2H_6) (although this 10 meV is within the resolution of the experiment). It should be noted that the entire spectrum, including features at lower energies, shifts downward together with the C-H stretch peak. Figure 7 demonstrates this, comparing Z_{eff} spectra for two of the alkanes. Spectra for propane (C_3H_8) and heptane (C_7H_{16}) are shown with the propane spectrum scaled up in magnitude by a factor of 60 and shifted downward in energy by 100 meV. The two spectra have remarkably similar shape over the entire experimental range. Both the shape of the C-H stretch resonance and the relative positions of the resonances remain approximately constant for all of the alkanes studied.

The magnitude of Z_{eff} increases rapidly with molecular size (Fig. 8). This was observed in earlier measurements for positrons at energies near room-temperature [16,26,29]. The present data show a similar rapid increase in the magnitude of the vibrational resonance peaks as molecular size increases. Figure 9 plots the ratios of the heights of the C-H stretch peaks to the room temperature values of Z_{eff}. The

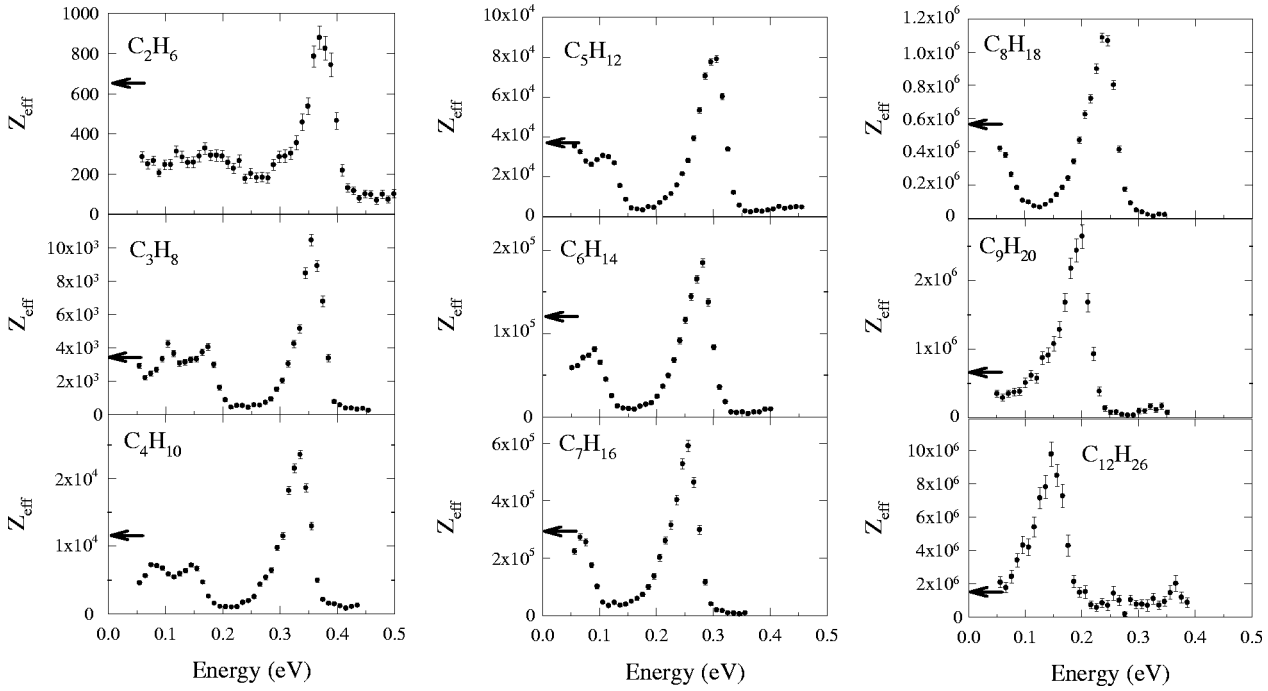

FIG. 5. Z_{eff} as a function of incident positron energy for the alkanes. Arrows on the vertical axis indicate Z_{eff} for a room-temperature thermal distribution of positrons.

height of the C-H stretch is a convenient indicator of the magnitude of the Z_{eff} spectrum. As can be seen in Fig. 5, the magnitudes of the lower energy features, where visible, are roughly proportional to the height of this C-H peak; so observations about scaling of the C-H peak are qualitatively correct for the rest of the spectrum. The height of the Z_{eff} peak associated with the C-H stretch is a factor of ~ 2 greater than the measured Z_{eff} for a room-temperature thermal distribution of positrons, Z_{eff} (300 K), for each of the alkanes up to eight carbons (Fig. 9). For nine and twelve carbons, this ratio jumps abruptly to ~ 5. A possible explanation for this will be discussed below.

B. Effects of fluorination on Z_{eff}

Changes in Z_{eff} (300 K) for partially fluorinated alkanes were investigated by Murphy and Surko [27] and later by Iwata *et al.* [18]. A general trend observed for alkanes with six or fewer carbons is that Z_{eff} increases with the first fluorine atom substituted, then decreases as more substitutions are made. In all cases studied, Z_{eff} for fully fluorinated alkanes is significantly smaller than the corresponding hydrogenated alkane.

It has been postulated that replacement of hydrogen atoms with fluorine in alkanes reduces the attraction of the positron to the molecule. This dependence on the number of fluorine atoms might then be explained by direct annihilation enhanced by a weakly bound or low-lying virtual state in the singly fluorinated molecule, which becomes unbound with

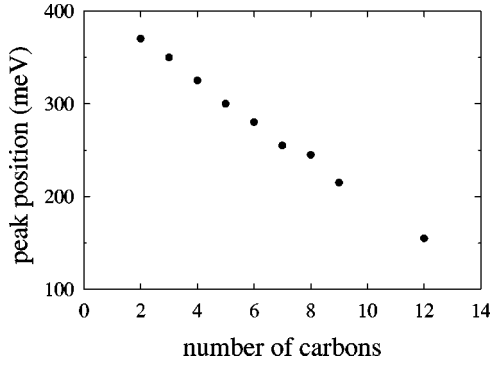

FIG. 6. Energy position of the C-H stretch peak for alkanes (C_nH_{2n+2}) as a function of number of carbon atoms (n). Methane (CH_4) exhibits no C-H stretch resonance.

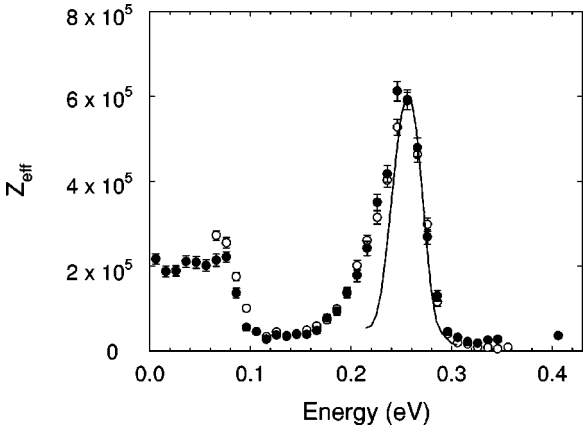

FIG. 7. Z_{eff} for propane (C_3H_8) (○) and heptane (C_7H_{16}) (●). The spectrum for propane has been scaled upward in magnitude by 60 and shifted downward in energy by 100 meV for comparison. The solid line shows the energy width of a typical positron pulse as measured using a retarding potential analyzer.

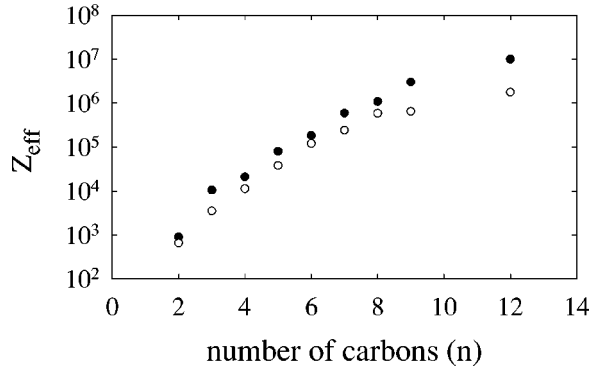

FIG. 8. Filled circles show the height of the peak in Z_{eff} attributed to the C-H stretch vibrational mode for alkanes as a function of number of carbon atoms. Open circles show Z_{eff} measured for a room-temperature distribution of positrons.

the addition of more fluorine [17,18].

Figure 10(a) compares Z_{eff} for hexane (C_6H_{14}) and for 1-fluorohexane ($C_6H_{13}F$). The substitution of just one hydrogen atom by a fluorine causes a tenfold reduction in the height of the C-H peak. Similar, though less dramatic, effects are seen in the spectrum of 1-fluorononane ($C_9H_{19}F$) [Fig. 10(b)]. Both molecules show an upturn in Z_{eff} for positron energies near 50 meV, the lower limit of the range of the experiment. It should be pointed out that, although the height of the C-H peak is greatly reduced by the substitution of one fluorine atom, the value of Z_{eff} for a room-temperature distribution is larger for 1-fluorohexane (269 000) than for hexane (120 000). [Z_{eff} (300 K) has not been measured for 1-fluorononane.] It is also interesting to note that, while height of the C-H stretch peak is reduced with fluorination, little change in the *position* of the peak is observed in 1-fluorononane.

C. Effects of molecular shape

As shown in Fig. 11, only slight differences are seen in the Z_{eff} spectra of isopentane [$CH_3CH_2CH(CH_3)_2$] and *n*-pentane [$CH_3(CH_2)_3CH_3$]. Above ~200 meV no significant variation is seen. Below 200 meV, isopentane has a slightly larger Z_{eff} (~15%), but the energy dependence is similar. Annihilation rates for these molecules have been reported previously and $Z_{eff}(300K)$ is 30% larger for isopentane than for *n*-pentane [30]. The present experiment samples

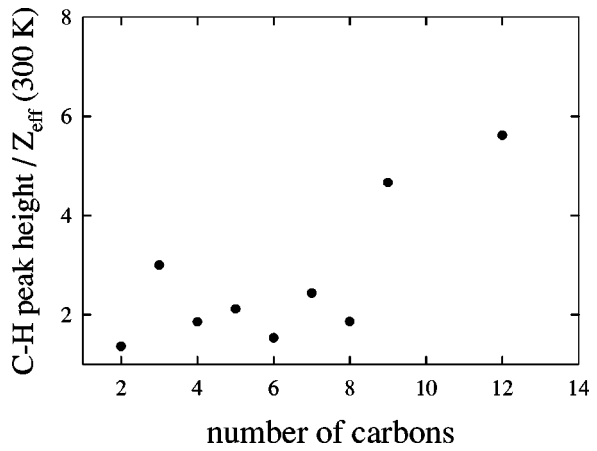

FIG. 9. The ratio of the C-H stretch peak height to Z_{eff} for room-temperature positrons for the alkanes as a function of the number of carbon atoms.

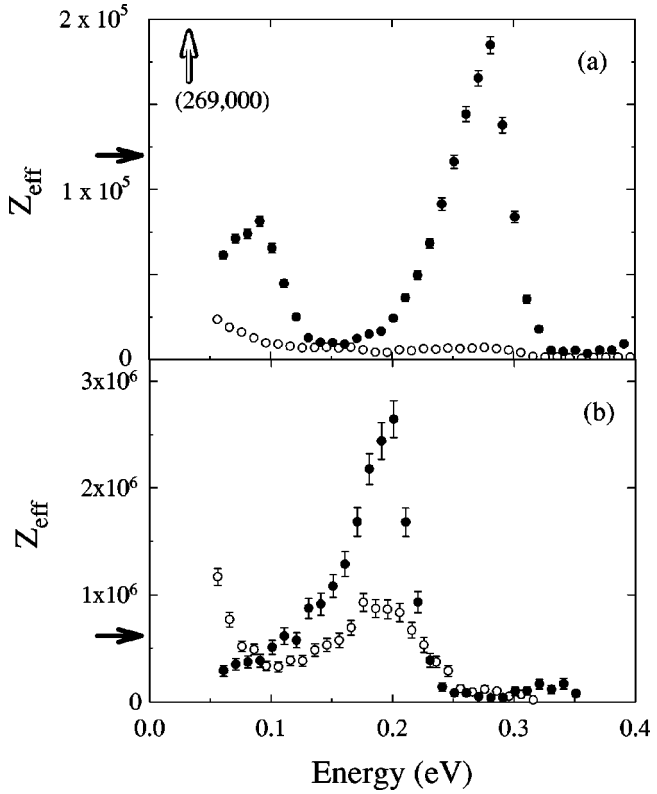

FIG. 10. Closed circles show the positron annihilation rates Z_{eff} for (a) hexane (C_6H_{14}) and (b) nonane (C_9H_{20}). Open circles show Z_{eff} for (a) 1-fluorohexane and (b) 1-fluorononane. Arrows on the vertical axis indicate Z_{eff} for a room-temperature distribution of positrons. In (a) the open arrow indicates the value for 1-fluorohexane.

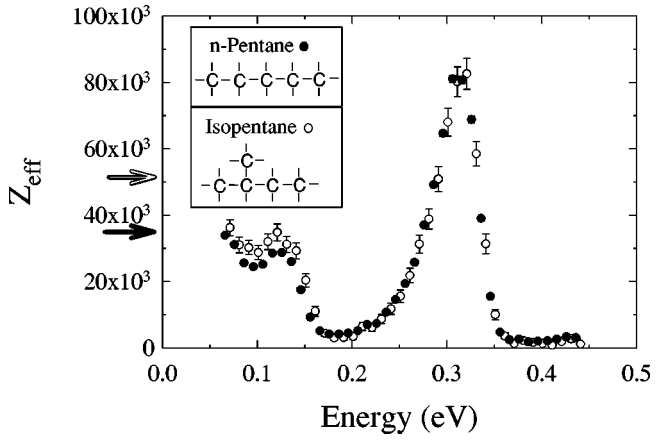

FIG. 11. Positron annihilation rates Z_{eff} for *n*-pentane (●) and isopentane (○). Arrows on the vertical axis indicate Z_{eff} (300 K) for the two molecules. The filled arrow indicates *n*-pentane. The open arrow indicates isopentane. The chemical structures of *n*-pentane and isopentane are shown in the inset.

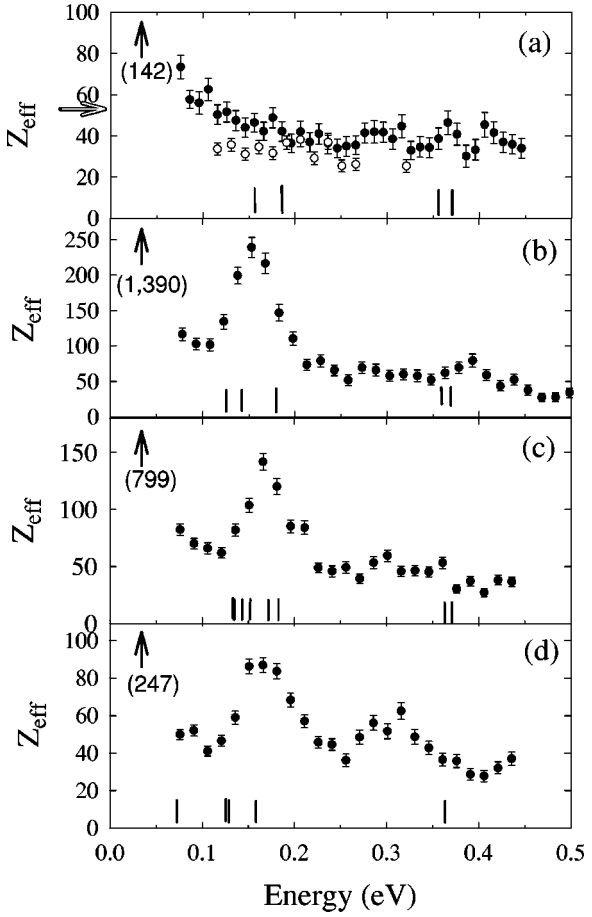

FIG. 12. Positron annihilation rates Z_{eff} for (a) methane (CH_4) and carbon tetrafluoride (CF_4), (b) methyl fluoride (CH_3F), (c) difluoromethane (CH_2F_2), and (d) trifluoromethane (CHF_3). Vertical lines indicate the energies of the vibrational modes. Arrows indicate Z_{eff} for a thermal distribution of positrons. In graph (a) the solid arrow refers to methane, the open arrow to carbon tetrafluoride.

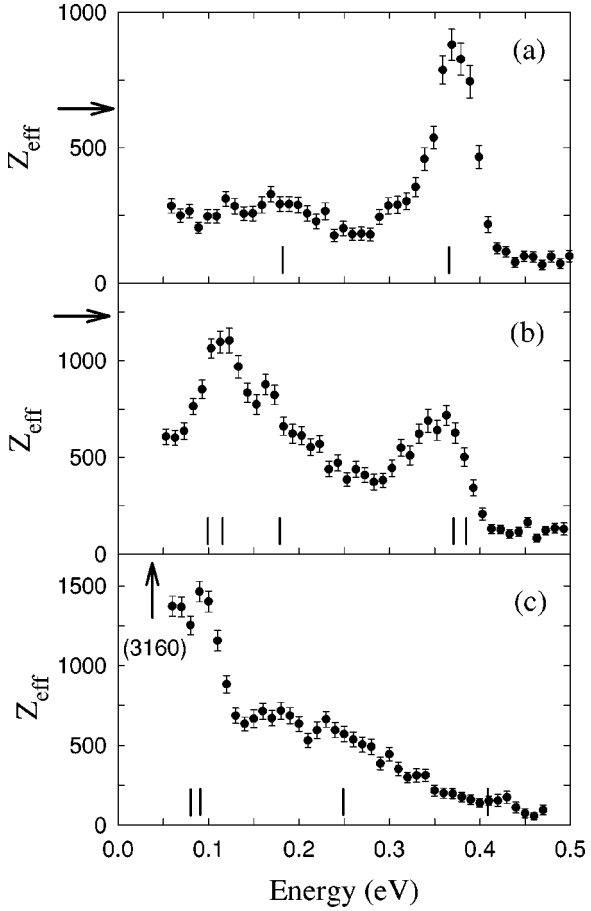

FIG. 13. Positron annihilation rates Z_{eff} for the two-carbon molecules, (a) ethane (C_2H_6), (b) ethylene (C_2H_4), and (c) acetylene (C_2H_2). Vertical bars indicate the energies of the strongest infrared active vibrational modes. Arrows indicate Z_{eff} for a Maxwellian distribution of positrons at 300 K.

very little of a room-temperature Maxwellian distribution so the results are consistent with those earlier measurements of Z_{eff} (300 K).

D. Smaller hydrocarbons and fluorocarbons

Molecules as large as those described above are difficult to treat theoretically. In order to test models of positron annihilation, it would be helpful to study smaller molecules with fewer degrees of freedom. Again, because of the high-energy, relatively isolated C-H stretch mode, small hydrocarbons were chosen as a starting point. Calculations for methane and acetylene, for example, have already been published [31].

Measurements of Z_{eff} for methane as well as for its fluorine-substituted equivalents ($CH_{4-x}F_x$) are shown in Fig. 12. Methane (CH_4) exhibits no large peaks within the range of our experiments, but fluorine substitution of methane introduces a peak near 150 meV. This low-energy resonance is observed in all partially fluorinated compounds, but not in CH_4 or CF_4.

Figure 13 shows the previously reported Z_{eff} spectra for ethane (H_3C-CH_3), ethylene ($H_2C{=}CH_2$), and acetylene ($HC{\equiv}CH$) [25]. The C-H stretch peak is slightly reduced in ethylene, and absent for acetylene, while lower energy modes as well as Z_{eff} (300 K) are observed to increase with the introduction of double and triple carbon bonds.

V. DISCUSSION

A. Large alkanes

In the context of the model by Gribakin [17], molecules with $Z_{eff} \geqslant 1000$ are predicted to have vibrational Feshbach resonances. This is observed for all alkane molecules larger than methane. In the larger alkanes, we interpret the difference between the energy of the resonance and the energy of the vibrational mode as the binding energy of the positron to the vibrationally excited molecule. When the energy of the incident positron plus the energy released by positron-molecule binding equals the energy of a vibrational mode of the molecule [Eq. (2)], a Feshbach resonance can occur between the free and bound positron states. This greatly increases the overlap of the positron and electron wave functions causing a large increase in the annihilation rate. Thus,

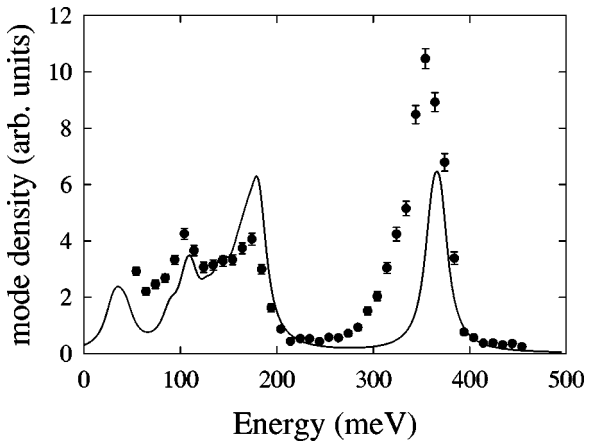

FIG. 14. The solid line shows the vibrational modes for propane represented as Lorentzian line shapes of width 10 meV. The Z_{eff} spectrum for propane (C_3H_8) is also shown (●) for comparison [32]. The relative scaling is arbitrary.

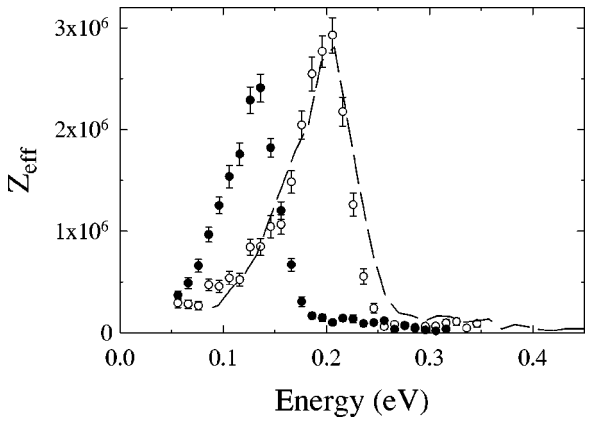

FIG. 15. Positron annihilation rate Z_{eff} as a function of incident positron energy for nonane (●) and nonane-d_{20} (○) in the range of energies $50 \leqslant \varepsilon \leqslant 450$ meV. Dashed line indicates Z_{eff} for nonane-d_{20} scaled for a reduced mass ratio, $\xi = 0.64$, and scaled in amplitude (by 1.167) to match the C-H peak for nonane.

the positions of peaks in the Z_{eff} spectra and the known vibrational mode energies of a molecule provide a measure of the binding energy of a positron to the molecule.

Figure 14 shows the spectrum of vibrational modes of propane, with each mode represented by a Lorentzian line shape of width 10 meV [32]. For the purposes of this simple calculation, all modes are given equal weight and no overtones are included. The similarity between the Z_{eff} spectrum and this simple linear mode spectrum may be an indication that initially, only single vibrational quanta are exchanged. The weight given to each mode for the purposes of predicting Z_{eff} should depend on the strength of the coupling between the mode and the positron and the lifetime of the quasibound state. By comparison with the experimental data, it appears that the C-H stretch modes receive greater weight than the lower energy modes.

The lifetime of this quasibound state may be increased by redistribution of vibrational energy among the normal modes of the molecule [33]. If either nonlinear, Coriolis, or centrifugal effect or the presence of the positron causes the vibrational energy to move into modes that couple weakly to the transition between free and bound positron states, the lifetime of the quasibound state may become long, further enhancing Z_{eff}. This energy redistribution is necessary for vibrational enhancement. Indeed, the number of simple C-H modes increases only linearly with the size of the molecule, and does not explain the exponential growth of Z_{eff} shown in Fig. 8.

Figure 4 showed the Z_{eff} spectrum for butane-d_{10} scaled by the reduced mass factor ξ for the stretch vibration of an isolated C-H pair. The fact that the peak shape remains approximately constant in the spectrum of the deuterium-substituted molecule (the slight increase in width can be attributed to scaling of the experimental beam resolution) indicates that either a single mode is involved, or that all modes involved have similar reduced mass ratios.

A careful examination of ξ provides more information about the specific vibrational mode excited. The scaling of the spectrum is complicated by the energy shift due to positron binding. If we attribute the shift to the positron-electron correlations that, within the present resolution, are not affected by small motions of the nuclei, deuteration is not expected to change the magnitude of the shift. Scaling only the mode energy, deuteration should cause the peak to appear at an energy $\Delta\epsilon = (E_{ex} - E_0)(1 - \sqrt{\xi})$ lower than for the hydrogenated molecule, irrespective of the magnitude of the energy shift. This energy shift with deuteration is observed to be $\Delta\epsilon = 80 \pm 5$ meV for both butane (C_4H_{10}) (Fig. 4) and nonane (C_9H_{20}) (Fig. 15), the only other molecule whose deuterated isotope was studied. Since we expect little change in the energy of the C-H stretch modes for the two molecules, this agreement is encouraging. In addition, the magnitude of the shift may be a signature of the excited mode. As stated earlier, the ξ factor can be calculated from the motion of the atoms in the mode. In highly symmetric modes in alkanes, the carbon atom moves very little so the reduced hydrogen (deuterium) mass is equal to its actual mass. This would make ξ exactly 0.5 and predict a shift of 105 meV. On the other hand, in a mode in which all of the hydrogen (deuterium) atoms move together, the momentum of each carbon atom must cancel the momentum of approximately two hydrogen (deuterium) atoms. Taking the atomic weight of carbon as 12 amu, this makes ξ equal to $[2/(12+2)]/[(12+4)/4] = 0.57$. For this type of mode, the predicted shift is 90 meV, which is much closer to the observed value of 80 meV.

Figures 8 and 9 show the close correlation between the magnitude of Z_{eff} (300 K) for a room-temperature distribution of positrons and Z_{eff} at larger energies. For the alkane molecules studied, the magnitude of Z_{eff} varies by nearly three orders of magnitude while the ratio of the Z_{eff} peak height to the thermal Z_{eff} remains approximately constant (i.e., within a factor of 2–6). This appears to us to provide compelling evidence that the same mechanism is responsible for both the enhancements in the present data and the large Z_{eff} values previously reported for a Maxwellian distribution of positrons at 300 K [18].

The low values of Z_{eff} (300 K) compared with Z_{eff} at the C-H stretch peak in alkanes of more than eight carbons also appears to be consistent with the energy-resolved Z_{eff}. This can be attributed to the depression in the Z_{eff} spectrum seen, for example, at 200 meV in the data for butane (Fig. 5). For nonane (C_9H_{20}), the C-H peak occurs at $\sim$200 meV. If the butane spectrum is shifted by the same amount as the C-H peak (i.e., 200 meV), this depression falls within the room-temperature energy distribution. Thus, the heights of all of the resonance peaks continue to increase, but, for more than eight carbons, the positron binding energy is larger than most of the low energy modes and Eq. (2) cannot be satisfied for most of the room-temperature distribution of positron energies. Consequently, the magnitude of Z_{eff} for room-temperature positrons lags behind the magnitude of the energy-resolved structure as indicated by the value of Z_{eff} at the C-H stretch peak.

B. Effects of fluorination on Z_{eff}

With regard to the effect of fluorination of molecules on Z_{eff}, the results point to a strong nonlocal effect. When a single fluorine was substituted at the end of the hydrocarbon chains, it reduced the magnitude of the C-H stretch peak by a factor of more than 2. If the wave function of the bound positron is distributed throughout the molecule and is affected strongly by the single fluorine, it must happen in a way that does not severely change the energy of the bound state. It could be that the presence of fluorine inhibits the redistribution of vibrational energy between modes, reducing the lifetime of the quasibound state. Another possible explanation is that the new inelastic channels involving vibration of the fluorine atom may provide an ''escape'' for the positron from the quasibound state, thus reducing both the lifetime of the state and Z_{eff}.

As indicated both in previous room-temperature experiments and in this energy-resolved study, fluorine substitution in both of the alkanes studied causes an increase in Z_{eff} at lower positron energies ($\sim$25 meV). This increase could be caused by enhancement of lower energy resonances or by the appearance of new resonances associated with the C-F bend or C-F stretch modes.

C. Effects of molecular shape

Although Z_{eff} (300 K) for *n*-pentane and isopentane are noticeably different (*n*-pentane, 37 800; isopentane, 50 500), we see only slight differences in the energy-resolved Z_{eff} spectrum in the range of our experiment (cf. Fig. 11). Since the C-H stretch mode causes little motion of the carbon atoms, we do not expect the character of the C-H stretch mode itself to change significantly between *n*-pentane and isopentane. Lower energy modes that *do* involve motion of the carbon atoms might be affected by the change in molecular shape, but most of these are outside the range of the present experiment. This may explain why the change in Z_{eff} (300 K) is accompanied only by small changes in the spectrum measured here.

D. Smaller hydrocarbons and fluorocarbons

In the fluorinated methane series, we see the first example of enhancements near some vibrational modes without enhancement near others. There appears to be no C-H stretch resonance in any of the molecules in Fig. 12, while three of the molecules show at least one resonance near 180 meV. The cause of this enhancement only near selected modes is not understood and is an important question in understanding this phenomenon. A study currently in progress is attempting to identify the mode or modes responsible for the observed enhancements of Z_{eff}.

In the two-carbon series (Fig. 13), we see the gradual disappearance of the C-H stretch resonance and the appearance of lower energy resonances as the strength of the carbon bond grows and the number of hydrogen atoms is decreased.

Although the data do not extend below 50 meV, we may draw some conclusions about the low energy Z_{eff} spectrum of the fluorinated methanes from a comparison with measurements using thermal positrons. When the values of Z_{eff} (300 K) are considered, it is apparent that, for all of the molecules except CF_4, there are features in the low energy Z_{eff} spectrum which are larger in magnitude than the resonant enhancements observed in the energy range of the current experiment. In particular, we may conclude that although the spectra for methane and carbon tetrafluoride have similar behavior in the range of the this experiment, they diverge for positron energies below 50 meV. One possible origin of this effect is the direct annihilation enhancement mechanism described by Gribakin [17].

VI. CONCLUDING REMARKS

We have presented detailed measurements of positron annihilation rates for a number of molecules resolved as a function of positron energy. In alkane molecules, these data show large vibrational resonance peaks that are down-shifted from the vibrational mode energies by an amount $\Delta\epsilon$, which increases with molecular size. These observations are consistent with a model by Gribakin that predicts large enhancements of Z_{eff} due to vibrational Feshbach resonances. The model requires the existence of positron-molecule bound states. We interpret the quantity $\Delta\epsilon$ as a measure of this binding energy. For alkane molecules, $\Delta\epsilon$ increases linearly with the number of carbons from ethane (C_2H_6) to dodecane ($C_{12}H_{26}$). Single fluorination of alkane molecules drastically reduces the annihilation rate at the C-H stretch mode even for fairly large alkanes, but appears to change the binding energy very little. Comparisons of pentane and isopentane indicate that changes in molecular shape had no effect on either the position, magnitude, or shape of Z_{eff} at the C-H stretch peak. We have plans to further investigate changes in the Z_{eff} with deuteration with emphasis on identifying the mode or modes responsible for the resonance peaks.

With regard to smaller molecules, methane and carbon tetrafluoride exhibit no resonances, although methyl fluoride, difluoromethane, and trifluoromethane do. Data for two-carbon hydrocarbons were presented showing that the progression from ethane ($H_3C–CH_3$) to ethylene ($H_2C=CH_2$), then to acetylene ($HC\equiv CH$) reduces the magnitude

of the C-H stretch peak, but enhances Z_{eff} at lower energies. We hope that these measurements will provide guidance for theoretical calculations of Z_{eff} for smaller molecules.

Generally speaking, measurements of $Z_{eff}(\varepsilon)$ for the larger alkanes are in reasonable agreement with the predictions of Gribakin's model. These results, taken together, provide evidence for positron binding to alkanes. There are, however, many issues that remain to be addressed. One such issue is making a closer connection between values of Z_{eff} (300 K) measured with room-temperature positrons and our measurements of $Z_{eff}(\varepsilon)$ at higher energies. Another important question is understanding the possible role of intramolecular vibrational energy redistribution in the annihilation process, particularly in larger molecules. Finally, there is the question of understanding the role of chemical structure in determining the magnitude and energy dependence of $Z_{eff}(\varepsilon)$.

In the area of annihilation in small molecules, the physical picture is, at present, less well developed. The annihilation rate in many small molecules is also much larger than expected on the basis of simple collisions. However, the magnitude of $Z_{eff}(\varepsilon)$ and changes in this quantity associated with changes in chemical composition are not understood. We would hope that quantitative $Z_{eff}(\varepsilon)$ spectra measured using the cold positron beam will motivate new calculations for small molecules. It is likely that these results, when compared with the data, will help to elucidate the operative annihilation mechanism in small molecules.

ACKNOWLEDGMENTS

We have benefitted greatly from extensive discussions with Gleb Gribakin. We are pleased to also acknowledge helpful conversations with James Sullivan, Joan Marler, Steve Buckman, Franco Gianturco, Jim Mitroy, Marco Lima, and Mineo Kimura and the technical assistance of Gene Jerzewski. This work was supported by National Science Foundation Grant No. PHY 98-76894, and the Office of Naval Research Grant No. N00014-02-1-0123.

[1] R. Ramaty and R.E. Lingenfelter, in *High Energy Astrophysics*, edited by J. Matthews (World Scientific, New York, 1994), p. 32.
[2] L.D. Hulett, Jr., D.L. Donohue, J. Xu, T.A. Lewis, S.A. McLuckey, and G.L. Glish, Chem. Phys. Lett. **216**, 236 (1993).
[3] L.D. Hulett, Jr., J. Xu, T.A. Lewis, O.H. Crawford, and S.A. McLuckey, Mater. Sci. Forum **175-178**, 687 (1995).
[4] P.J. Schultz and K.G. Lynn, Rev. Mod. Phys. **60**, 701 (1988).
[5] *Positron Spectroscopy of Solids*, edited by A. Dupasquier and A.P. Mills, Jr. (IOS Press, Amsterdam, 1995).
[6] M. Charlton and J. Humberston, *Positron Physics* (Cambridge University Press, New York, 2001).
[7] *New Directions in Antimatter Chemistry and Physics*, edited by C.M. Surko and F.A. Gianturco (Kluwer Academic Publishers, Dordrecht, 2001).
[8] E.P. da Silva, J.S.E. Germano, and M.A.P. Lima, Phys. Rev. Lett. **77**, 1028 (1996).
[9] G. Laricchia and C. Wilkin, Phys. Rev. Lett. **79**, 2241 (1997).
[10] G. Laricchia and C. Wilkin, Nucl. Instrum. Methods Phys. Res. B **143**, 135 (1998).
[11] J. Mitroy, M.W.J. Bromley, and G. Ryzhikh, J. Phys. B **32**, 2203 (1999).
[12] G.G. Ryzhikh and J. Mitroy, J. Phys. B **33**, 2229 (2000).
[13] D.A.L. Paul and L. Saint-Pierre, Phys. Rev. Lett. **11**, 493 (1963).
[14] V.I. Goldanskii and Y.S. Sayasov, Phys. Lett. **13**, 300 (1964).
[15] P.M. Smith and D.A.L. Paul, Can. J. Phys. **48**, 2984 (1970).
[16] C.M. Surko, A. Passner, M. Leventhal, and F.J. Wysocki, Phys. Rev. Lett. **61**, 1831 (1988).
[17] G.F. Gribakin, Phys. Rev. A **61**, 022720 (2000).
[18] K. Iwata, G. Gribakin, R.G. Greaves, C. Kurz, and C.M. Surko, Phys. Rev. A **61**, 022719 (2000).
[19] S.J. Gilbert, C. Kurz, R.G. Greaves, and C.M. Surko, Appl. Phys. Lett. **70**, 1944 (1997).
[20] C. Kurz, S.J. Gilbert, R.G. Greaves, and C.M. Surko, Nucl. Instrum. Methods Phys. Res. B **143**, 188 (1998).
[21] J.P. Sullivan, S.J. Gilbert, and C.M. Surko, Phys. Rev. Lett. **86**, 1494 (2001).
[22] J.P. Sullivan, J.P. Marler, S.J. Gilbert, S.J. Buckman, and C.M. Surko, Phys. Rev. Lett. **87**, 073201 (2001).
[23] J.P. Sullivan, S.J. Gilbert, J.P. Marler, R.G. Greaves, S.J. Buckman, and C.M. Surko, Phys. Rev. A **66**, 042708 (2002).
[24] S.J. Gilbert, J.P. Sullivan, R.G. Greaves, and C.M. Surko, Nucl. Instrum. Methods Phys. Res. B **171**, 81 (2000).
[25] S.J. Gilbert, L.D. Barnes, J.P. Sullivan, and C.M. Surko, Phys. Rev. Lett. **88**, 043201 (2002).
[26] G.R. Heyland, M. Charlton, T.C. Griffith, and G.L. Wright, Can. J. Phys. **60**, 503 (1982).
[27] T.J. Murphy and C.M. Surko, Phys. Rev. Lett. **67**, 2954 (1991).
[28] R.G. Greaves and C.M. Surko, Phys. Plasmas **4**, 1528 (1997).
[29] K. Iwata, R.G. Greaves, T.J. Murphy, M.D. Tinkle, and C.M. Surko, Phys. Rev. A **51**, 473 (1995).
[30] K. Iwata, R.G. Greaves, and C.M. Surko, Phys. Rev. A **55**, 3586 (1997).
[31] F.A. Gianturco, T. Mukherjee, T. Nishimura, and A. Occhigrossi, in *New Directions in Antimatter Chemistry and Physics*, Ref. [7], pp. 451–474.
[32] G. Gribakin (private communication); the vibrational energies were computed by Peter Gill using the Q-CHEM program, see J. Kong *et al.*, J. Comput. Chem. **21**, 1532 (2000).
[33] G. Gribakin, in *New Directions in Antimatter Chemistry and Physics*, Ref. [7], pp. 413–435.